Free-form structures from topologically interlocking masonries

Vianney Loing, Olivier Baverel, Jean-François Caron, Romain Mesnil

Free-form structures from topologically interlocking masonries

Vianney Loing[a], Olivier Baverel[a], Jean-François Caron[a,*], Romain Mesnil[a]

[a]*Laboratoire Navier, UMR 8205, École des Ponts, IFSTTAR, CNRS, UPE, Marne-La-Vallée, France*

Abstract

The paper presents new results about the geometry of topological interlocking masonries and some possibilities they present to build without formwork. Construction without the use of formwork may be an important issue concerning both productivity increase and decreasing of waste generated on a construction site. Due to the development of computational design and robotics in the construction industry, it makes sense to (re)explore innovative design and process of complex masonry structures. The design of this kind of masonry is standard for planar structures, and in this paper, a generalization is proposed for the parametric design of curved structures. To achieve this, a criterion for translationally interlocked structure based on quadrilateral meshes is exhibited. The application of this criterion is then extended to masonry structures derived from other patterns. Physical prototypes of topological interlocking masonry are also presented. One of these designs seems to allow construction without formwork.

Keywords: Constructive geometry, Architectural geometry, Free-form, Topologically interlocked material, nexorade, PQ-mesh

1. Introduction

For the past 20 years, productivity growth in the construction sector has been only 1 % per year, while it is 2.8 % in the global economy and 3.6 % for the manufacturing industry. For developed countries, such as France or the United States, this productivity is even stagnant [1]. Among the seven progress tracks cited by Mckinsey2017 to improve productivity is the use of automation and digital technologies, including on-site construction with robotics. Several national and international initiatives projects have been launched, ETN European project (InnoChain[1]), in Switzerland (dfab[2]) or in France for instance (DiXite[3], Projet Matrice[4]).

But one has to keep in mind that robotisation of construction is not a new idea. Bock and Langenberg [2] remind us that following the Second World War attempts to industrialize the construction process appeared to face the challenge of reconstruction. This included prefabrication, standardization and site structuring. The oil crisis of 1973 was the reason for momentum in the West but not in Asia, especially in Japan, where the development of robots performing construction tasks is now a commercial reality (Sekisui House, Toyota House...).

To be competitive, the use of robots must propose an added value, and not just a substitute for traditional working force, difficult to compete with. Consequently, structural designs and process have to be revisited and adapted to the digital workflow. This work proposed such an approach and focuses on the robotic construction of masonry - i.e. constructions composed of blocks (bricks, stones, concrete, etc.) whether or not joined by a binder. This problem is not new either (see Fig. 1), studied by various research teams (including Gramazio and Kolher in Zurich [3] or the Chair of Building Realization and Robotics in Munich), and some companies already offer commercial products for stacking bricks with robot arms (Construction Robotics or Fastbrick among others).

Several challenges for the digital fabrication of masonry structures can be identified. First, the in-situ fabrication requires robust techniques to localise components, as a construction site is an unstructured environment, with much more variability than a factory or a lab. In a previous paper [4] we present the part of this research concerning the construction process and robotics aspects. These first results permit a robot to localize and manipulate an object (stone or brick) accurately, using scene views from uncalibrated cameras (adaptation to worksite environment), and using a Convolutional Neural Networks (CNN) trained using hundreds of thousands of synthetically rendered scenes with randomized parameters. The objective is to permit the robot to recognize and manipulate very different masonry components (a severe task for a worker), and also to ask it to hold the structure if necessary, as a formwork would usually do.

The second challenge is to construct structurally sound masonry structures by keeping a dry construction pro-

*Corresponding author
E-mail: jean-francois.caron@enpc.fr

[1] http://innochain.net/
[2] http://www.dfab.ch/
[3] https://dixite.future-isite.fr/
[4] http://www.matrice-impression3d.fr/projet/

Figure 1: T. Bock, ESPRIT 3 6450 ROCCO 1992 [2]

cess. Indeed, a ubiquitous method to obtain reliable masonry structures is to use hollow masonry blocks as a lost formwork and pour concrete after the introduction of reinforcements inside. So far, this is also one of the most common techniques to reinforce 3d printed structures. Although this technique is very common, it requires additional assembly sequences and time and perhaps more importantly, it prevents the disassembly of the structure and most chance of reuse of the components.

This article focuses on the construction of masonry structures with good mechanical properties (out-of-plane resistance and ductility) without the need for additional reinforcements, which is a major issue in additive manufacturing processes. Non-vertical elements, like arches or floors, are studied more precisely, in an exploration of how computational design and robotics may be a way to build decreasing or suppressing the use of formwork and temporary structures. It is a very important issue concerning both productivity and amount of generated waste. For instance, at Hong Kong in 2013, approximately 3,591 tonnes of construction waste were disposed of daily, representing 25% of total solid waste received at landfills [5]. Moreover, the fabrication and construction of these formworks, represent 35% - 60% of the total concrete work cost [6].

This article details the design structural choices and the parametric design investigated to reduce the need for formwork, re-exploring the work of master builders. Auguste Choisy, for example, [7] expose the principles of construction of Byzantine vaults without formwork. A classic way to build a vaulted ceiling, using a wooden frame, is to proceed row by row and once the keystone putting in place, to remove the frame (Fig.2a). To achieve such a building without formwork, the Byzantines proposed instead of building row by row, to build arches by arches. Slightly inclined to help cohesion, the arches are achieved one by one and rest on one another (Fig.2b). Other more recent researches propose to limit the use of formwork by changing also the erection strategies [8, 9].

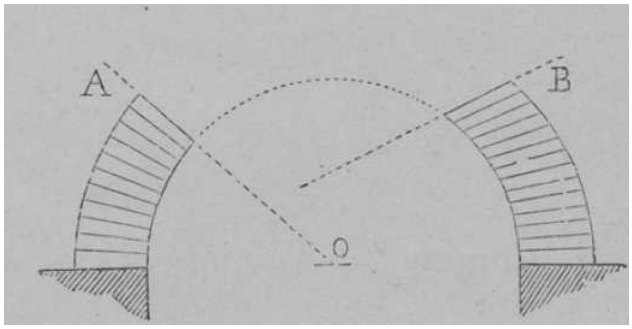

(a) A classical strategy using keystone and formwork.

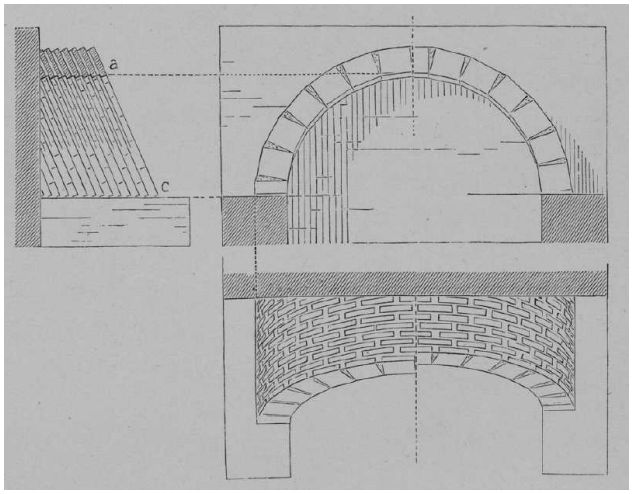

(b) Byzantine strategy, without formwork.

Figure 2: Construction of a vault ceiling, with and without formwork [7]

To go further, that is easy to understand that the shape of the block itself may help to the stability of the stack. *Stereotomy* is the art of cutting solids, generally stones, and was widely used in the former centuries to build complexes structures such as vaults and arches, using only small elements. But this art fell into disuse with the emergence of new materials such as concrete or steel and with the introduction of the elasticity theories. However, since a few years, the interest in these old techniques was renewed thanks to Computer-Aided Design tools such as parametric design software and robotic tooling. The proposal here is based on an innovative stereotomy from the 18$^{\text{th}}$ century, the flat vault of engineer and architect Joseph Abeille (Fig. 3). It allows covering a space using small similar elements with no keystone, nor glue. It represents a strong advantage today, particularly from an environmental point of view, since the structure could thus be disassembled and blocks easily reused. This vault is one example of what is called *topological interlocking assemblies* in the materials science community. These kind of assemblies have some interesting properties. For example, they can bear tensions and consequently bending

moments; not using mortar helps to avoid crack propagation [10, 11], and even though the assembly is made of brittle material, the behaviour of the system appears as ductile [12, 13, 14, 15, 16, 17, 18].

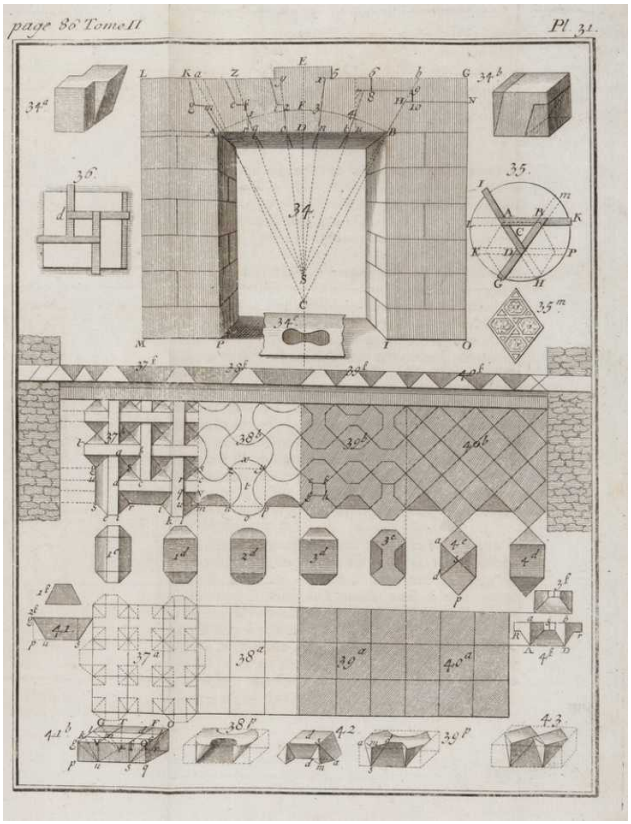

Figure 3: Abeille (37) and Truchet (38) flat vaults [19]. Some reciprocal structures can be noticed in (35) et (36).

Common examples of topological interlocking assemblies are the ones made from tetrahedrons, cubes [20] or the so-called osteomorphic block [13]. Several applications could be considered for the construction sector – earthquake resistance, paving [21], retaining walls [22, 23] – and recent examples in construction and architecture, mainly as prototypes, include [24, 25, 26].

Indeed, different procedures exist to create interlocking assemblies. [27] starts with a simple shape (for example, an Abeille flat vault) and deform it thanks to modifiers. [25] use techniques similar to the design process of reciprocal frames. [10, 28] link planes to the edges of regular lattices and tilt them (see Sec. 2) to obtain flat assemblies of convex polyhedra. This process is named by its authors *moving cross-section procedure* and allows to verify at the same time the concrete interlocking property of the assembly. This procedure is generalized to meshes of curved surfaces but without checking the interlocking property of the assembly [29] or without keeping convex blocks [30]. Indeed, using the moving cross-section procedure to design curved interlocking assemblies from non-regular lattices – eventually with variable tilt angle values – do not guarantee the interlocking. A simple mathematical criterion is proposed here ensuring that each block is indeed locked and allowing to check that all the assembly is interlocked.

After introducing the framework and some definitions, this criterion (a set of inequalities to satisfy) is detailed. Topologically interlocked masonries with variable inclination joints are described and designed from Planar Quadrangular (PQ) meshes of curved surfaces. Prototypes are presented, one of them is inspired by the Byzantine method of building vault. It could be built without the use of any formwork despite tensile stress hoops due to self-weight.

2. Topologically interlocked curved structures

Several definitions are proposed for topological interlocking [11, 12] but the one retained here comes from [28]: *In an assembly of elements, an element is* translationally locked (resp. rotationally locked), *if it can not be removed by translation (resp. rotation), provided its neighbours are considered as fixed. An assembly of N elements is translationally interlocked (resp. rotationally interlocked) if all its N elements are translationally locked (resp. rotationally locked). An assembly is* fully interlocked *if it is both translationally interlocked and rotationally interlocked.* In our work, we mainly focus on the translational interlocking of curved structures, how to obtain them and how to check their effective interlocking.

This approach can be thought of as a kinematic approach in yield design theory [31]. We postulate kinematically admissible displacement fields and check the resistance of the structure. The Upper bound theorem states that the given load factor is superior to the actual load factor. The case of interlocked masonries does not consider an external load, unlike equilibrium-based methods [32], which provide stable solutions for only one load case. The kinematic method is dual to an equilibrium-based approach, which looks for stress fields satisfying equilibrium and resistance constraints. In that case, the maximal load factor is a lower estimate of the actual load factor at yield. The complementary use of both methods indicates the accuracy of the estimation provided by both methods. Finally, the translational interlocking criterion is considered to provide structural ductility, even with brittle materials, which is one of the most interesting design features of topologically-interlocked materials.

For the geometrical construction of the topologically interlocked structure studied here, the moving cross-section procedure [28] is used. This classical method permits to build from a planar and regular mesh, and from the choice of a set of tilting angles $+\alpha$, an interlocked system constituted by blocks (regular tetrahedrons, which can be truncated by planes) and known as an Abeille flat vault and represented in Fig. 3: impossible to remove one block without moving the other blocks surrounding it.
Here the procedure is generalized to non regular lattices, with varying tilting angles and curved surface. Such research was also conducted in [29], but the focus is made

here on the use of PQ meshes (Fig. 4) which are commonly used in architectural applications [33, 34, 35] and on the definition of a mathematical criterion for interlocking.

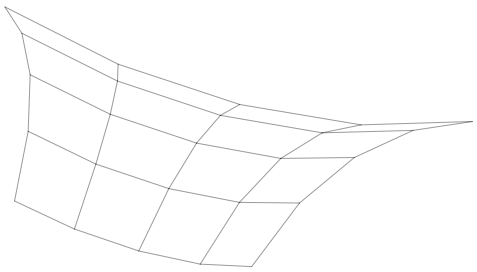

Figure 4: Example of a PQ mesh of a curved surface

F_1 and F_2 are two planar quadrangles (2 faces) of this mesh (Fig. 4), $\vec{n}_{F1}$ and $\vec{n}_{F2}$ their unit normal vectors. The edges of faces are numbered by subscripts i with $i \in \{1, 2, 3, 4\}$. For each face, four Planes P_i define the tetrahedron i (block i), their normal vector are $\vec{n}_i$ making a tilting angle α_i with $\vec{n}_{F1}$ or $\vec{n}_{F2}$ (Fig. 5).

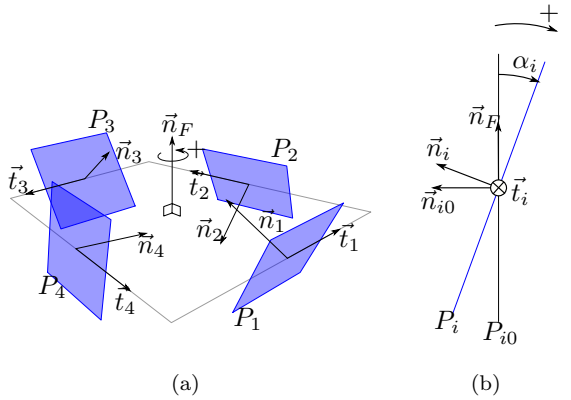

(a) (b)

Figure 5: Notations

The block V^{F_1} is generated from face F_1 and planes $\left\{P_1^{F_1}, P_2^{F_1}, P_3^{F_1}, P_4^{F_1}\right\}$. V^{F_2} is generated from face F_2 and planes $\left\{P_1^{F_2}, P_2^{F_2}, P_3^{F_2}, P_4^{F_2}\right\}$. Since V^{F_1} and V^{F_2} are neighbours, they share a common plane, for instance $P_1^{F_1} = P_3^{F_2}$. Except for periphery blocks, this remark stays valid for every block $P_i^{F_2}$. Therefore, for each block, the four common planes of the four neighbours, may or may not preclude every translational movement in all directions.
The generalization of the moving cross-section procedure to PQ mesh is not more detailed in this paper but a result represented on figure 6.

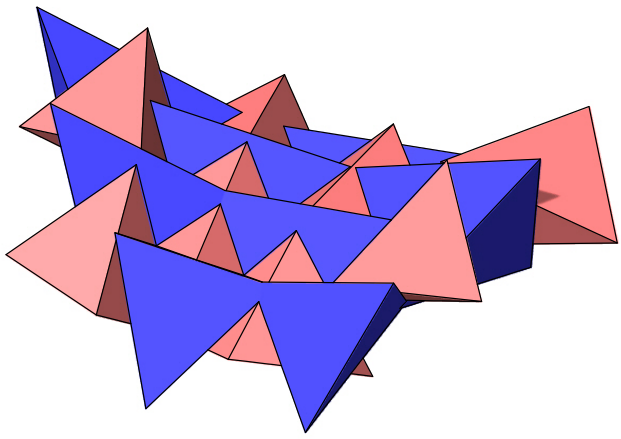

Figure 6: Generation of tetrahedron interlocked assembly on a curved surface. Here, the tilting angles are the same for each edge, which is just a particular case.

It might be necessary to truncate the blocks with planes parallel to the quadrangle plane if, for example, tetrahedrons partially overlap.
Truncate the blocks can also serve other purposes (see also [29, 36]) and may propose interesting solutions with or without voids or holes, with different reference planes (Fig. 7) and architectural effects. The last case (Fig. 7c) is visually similar to some nexorades based on quadrilateral meshes of beams [37], this comes as no surprise since topologically interlocked structures and nexorades are based upon similar structural principles.

3. Geometric conditions for an effective translational interlocking in a quadrilateral mesh

When building blocks from a PQ-mesh with variable inclination joints with the method presented before, the interlocking property of the blocks is not guaranteed. In this section, mathematical conditions (set on inequalities) on the normals of the planes used to build the interlocking blocks are presented. These conditions thus allow to verify that a block is effectively translationally interlocked, which is of great interest for assembly and structural reliability.
Consider a block V (Fig.8 in red) generated from planes P_1, P_2, P_3 and P_4 (the subscript F is no longer mentioned for better clarity) and $\vec{u}$ a displacement vector of this block. Since P_i also corresponds to the surface of the blue neighbour block, if the component of $\vec{u}$ along $\vec{n}_i$, the normal vector (see fig.5), is negative (i.e. $\vec{u}.\vec{n}_i < 0$), block V collides with its neighbour (Fig.8b). Conversely, if the component of $\vec{u}$ along $\vec{n}_i$ is positive (i.e. $\vec{u}.\vec{n}_i > 0$), the block movement is possible along $\vec{u}$ (Fig. 8a).
Therefore, plane P_i whose normal is $\vec{n}_i$ precludes translational movement of block V along $\vec{u}$ if and only if $\vec{u}.\vec{n}_i < 0$. And the displacement of block V along $\vec{u}$ is not possible, if and only if, at least one of the four planes P_1, P_2, P_3 or

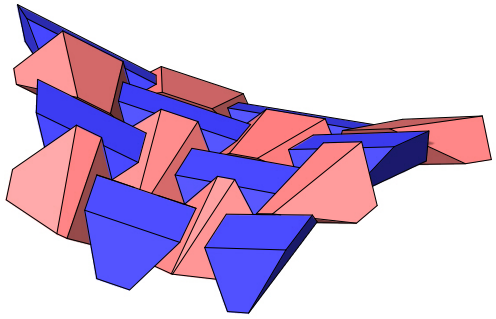

(a) Symmetric truncature

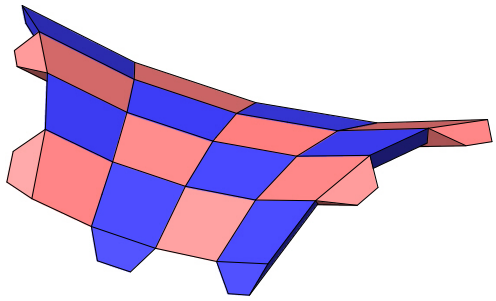

(b) a face plane and a resulting smooth surface

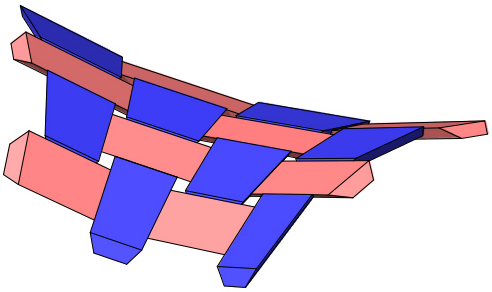

(c) a face plane and holes

Figure 7: The assembly Fig. 6 trimmed by different planes

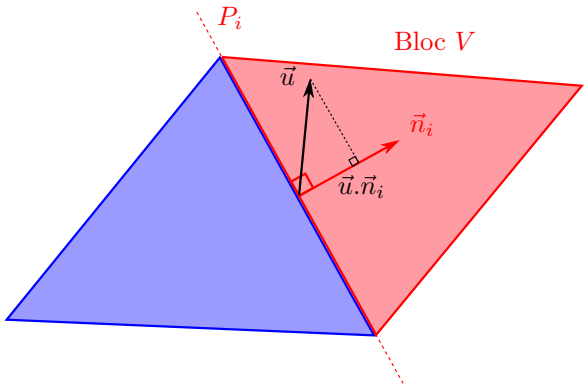

(a) The displacement of block V along $\vec{u}$ is possible ($\vec{u}.\vec{n}_i > 0$).

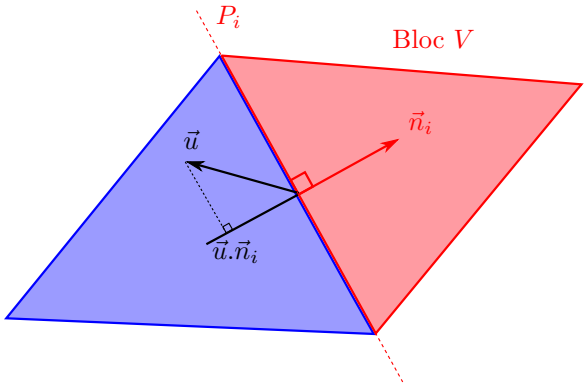

(b) The displacement of block V alongn $\vec{u}$ is impossible. The block collides indeed with its neighbour ($\vec{u}.\vec{n}_i < 0$).

Figure 8

P_4 precludes it. A necessary condition to have a translationally interlocked block is given in equation (1).

$$\forall \vec{u} \in \mathbb{R}^3, \begin{cases} & \vec{u}.\vec{n}_1 & < & 0 \\ \text{or} & \vec{u}.\vec{n}_2 & < & 0 \\ \text{or} & \vec{u}.\vec{n}_3 & < & 0 \\ \text{or} & \vec{u}.\vec{n}_4 & < & 0 \end{cases} \tag{1}$$

Conversely, block V is not translationally interlocked, if and only if there exists at least one displacement $\vec{u}$ which is not precluded by any of the four planes P_1, P_2, P_3 and P_4, this condition is summed up in (2).

$$\exists \vec{u} \in \mathbb{R}^3, \begin{cases} & \vec{u}.\vec{n}_1 & \geq & 0 \\ \text{and} & \vec{u}.\vec{n}_2 & \geq & 0 \\ \text{and} & \vec{u}.\vec{n}_3 & \geq & 0 \\ \text{and} & \vec{u}.\vec{n}_4 & \geq & 0 \end{cases} \tag{2}$$

The two equations (1) and (2) are therefore a criteria to check the locking of a block. However, a major inconvenient of this formulation is that, to prove that a block is translationally interlocked, one has to check the inequality on the right **for every** displacement $\vec{u}$. An equivalent and alternative proposal for the necessary condition satisfied by a block to be translationally interlocked is the set of equations (3):

$$\begin{cases} & det\left(\vec{n}_1, \vec{n}_2, \vec{n}_3\right) \cdot det\left(\vec{n}_1, \vec{n}_2, \vec{n}_4\right) < 0 & \text{(i)} \\ \text{and} & det\left(\vec{n}_1, \vec{n}_2, \vec{n}_3\right) \cdot det\left(\vec{n}_2, \vec{n}_3, \vec{n}_4\right) < 0 & \text{(ii)} \\ \text{and} & det\left(\vec{n}_1, \vec{n}_2, \vec{n}_3\right) \cdot det\left(\vec{n}_3, \vec{n}_1, \vec{n}_4\right) < 0 & \text{(iii)} \end{cases} \tag{3}$$

With $det\left(\vec{n}_1, \vec{n}_2, \vec{n}_3\right)$ the determinant of the vector $\vec{n}_1$, $\vec{n}_2$ and $\vec{n}_3$. System (3) allows to prove that a block is translationally interlocked, without the need to check an inequality for each $\vec{u}$. Note that these inequalities only depend of the normals $\vec{n}_1$, $\vec{n}_2$, $\vec{n}_3$ and $\vec{n}_4$, and are independent of the type of quadrangle, planar or not, from which it is generated (let's just assume that $det\left(\vec{n}_1, \vec{n}_2, \vec{n}_3\right) \neq 0$). The complete demonstration of System (3)is proposed in annex Appendix A.

Equation (3) implicitly depends on the shape of the quadrilateral, which can be considered as a design input, and on the angles of orientation, which are here considered as design variables. The determinants appearing in equation (3) create a coupling that is similar to the one observed in the planarisation of quadrilateral facets: it is difficult to solve directly, as it is non-convex.

4. Generalisation to other meshes

Although the quadrilateral meshes present an undeniable interest for architectural applications, and as such, have been the main topic of research in the architectural geometry community, the architects and engineers can select other mesh typologies, like hexagonal meshes. The proof for equation 3 allows to generalise the statement made in the previous part to such irregular meshes. The minimal number of planar contact to translationally interlock a block is four, and as a consequence, block arrangements derived from triangular meshes or mesh containing triangular facets cannot be fully translationally interlocked. A sufficient condition for a block to be translationally interlocked is to have four planar contacts satisfying equation (3). For each face with N facets, the interlocking condition can be rewritten as a set of $\binom{N}{4}$ equations. A block is topologically interlocked if the following condition is fulfilled:

$$\exists \{i, j, k, l\}, i \neq j \neq k \neq l$$
$$\begin{cases} & det\left(\vec{n}_i, \vec{n}_j, \vec{n}_k\right) \cdot det\left(\vec{n}_i, \vec{n}_k, \vec{n}_l\right) < 0 & \text{(i)} \\ \text{and} & det\left(\vec{n}_i, \vec{n}_j, \vec{n}_k\right) \cdot det\left(\vec{n}_j, \vec{n}_k, \vec{n}_l\right) < 0 & \text{(ii)} \\ \text{and} & det\left(\vec{n}_i, \vec{n}_j, \vec{n}_k\right) \cdot det\left(\vec{n}_k, \vec{n}_i, \vec{n}_l\right) < 0 & \text{(iii)} \end{cases} \tag{4}$$

This condition is sufficient, but not necessary, since the locking could be provided by more than four blocks in some peculiar situations. Although restricted, the condition provided by equation (4) is already much more complex to check than equation (3) for quadrilateral meshes. Equation (4) can be checked for any set of four planes among the N planes bonding a block, wich means that there are $\binom{N}{4}$ arrangements to check. For example, for a hexagon, there are $\binom{6}{4} = 15$ possible arrangement of interlocking planes. This surely provides much more redundancy in interlocking assemblies derived from hexagonal meshes, but also makes the design procedure more complex. A practical simplification could be to provide templates for families of meshes proposing a set of four planes that have to fulfill the interlocking condition (3) to the designer. Such examples are proposed for different meshes in Figure 9: the colored dotted lines correspond to the position of the planes used to create interlocking, other planes are either unconstrained or can provide additional interlocking and structural redundancy.

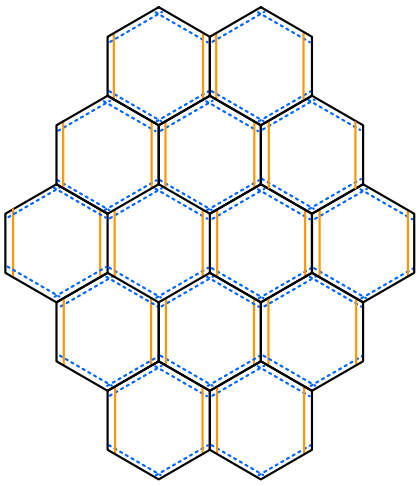

Figure 9: Set of planes used to create interlocking in a hexagonal mesh (blue dotted) and planes that can provide additional interlocking (orange)

5. Free-edges and interlocked structures

The reasoning pursued on the generalisation of the concept of translational interlocking to n-gons can also be applied to blocks on free edges. This question is crucial in many architectural applications, which feature openings. Figure 10 displays the topology of a mesh that can be used to generate corollas, as discussed in Section 8: the free-edge is depicted in light grey. Like in this figure, a block located on the boundary of a quadrilateral mesh only has three neighbours, which is not sufficient to provide translational interlocking. The stability can be ensured either by the construction of a bespoke ring that constraints the blocks, or by a mechanical attachement, like glueing [5] or by applying a pre-stress that prevents the mechanisms. The pre-stress can be active, for example through a cable, or passive, for example if the direction of extraction is pointing upwards and if the block is never subject to uplift, which is a reasonable assumption for masonry structure.

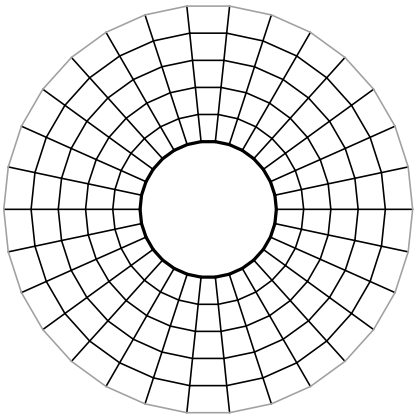

Figure 10: Top view of a quad mesh for a corolla, blocks adjacent to a free edge (light grey) only have three contacts

Nonetheless, it is possible to modify the mesh to introduce true topological interlocking. For example, one can merge adjacent quadrilaterals to create a pentagon with one free edge and four contact planes with its neighbours: this technique is illustrated in Figure 11. This strategy brings several potential complications which are not in the scope of this article: since the pentagonal facets are not planar and might thus be harder to manufacture and the assembly sequence of the pentagonal hoop might require a complex assembly kinematic where all the blocks would have to be installed at once. These limitations could be adressed with specific strategies, for example if the quad mesh is aligned with principal curvature directions then the resulting pentagon could easily be planarised [38]: several morphological strategies have been developed in the last decade for that purpose [39, 40].

[5] http://aauanastas.com/project/stone-matters/

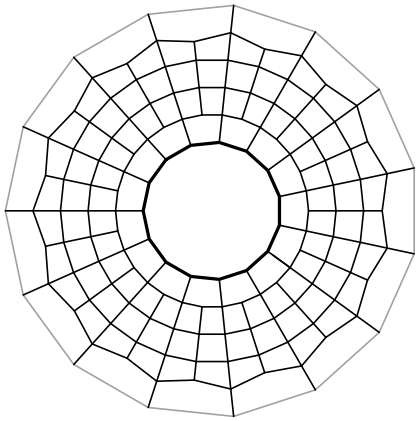

Figure 11: Top view of a quad mesh for a corolla with modification, blocks adjacent to a free edge (light grey) only have four contacts and topological interlocking is possible.

6. Design space for topologically interlocked masonries

A necessary condition to create translationally interlocked masonries has been proposed in this article. It is based on inequality constraints and might be unsual to work with for practitioners like architects or engineers. In the spirit of recent work on architectural geometry, this section discusses available degrees of freedom and highlights a geometrical transformation that preserves topologically-interlocked masonries. Two complimentary point of views are taken. First we consider a fixed geometry, while plane orientations are the design variables. Second, we consider a fixed plan orientation, while the position of the vertices of the reference mesh are the design variables.

First, the number of degrees of freedom can also be estimated when considering a fixed reference mesh and considering only the plane orientation as design variables. Equation (4) can be solved by fixing $\vec{n_1}$,$\vec{n_2}$ and $\vec{n_3}$ and by solving in $\vec{n_4}$ (the inequality becomes a linear inequality and defines thus a conical constraint for $\vec{n_4}$). The number of degrees of freedom is thus at least proportional to the number of facets in a quad mesh.

$$d_{interlocking} \sim F$$

For a k-gonal mesh, the number of degrees of freedom can be estimated with the same reasoning.

$$d_{interlocking} \sim (k-3)F$$

So that the ratio r between the number of variables E and the dimension of solution is approximately

$$r_{interlocking} \sim \frac{2k-6}{k}$$

There are no solution for triangular meshes, and the dimensionality of possible interlocking configurations increases with the average number of edges per facet in

the mesh. This is in accordance with common sense of masonry builders: brick patterns derived from hexagonal meshes are much more stable than those derived from quadrilateral meshes. To give a comparison with planarisation of a k-gonal mesh, which is a usual problems in architectural geometry used to benchmark numerical methods, there are $3V$ parameters and $(k-3)F \sim \frac{(2k-6)}{k-2}V$ planarity constraints [41], which gives an estimate of the dimension of the space of solutions.

$$d_{planarisation} \sim \frac{k+3}{k-1}V$$

The ratio r between the number of variables $3V$ and the dimension of solution is approximated by:

$$r_{planarisation} \sim \frac{k+3}{3\cdot(k-1)}$$

Using simple estimates, the difficulty of finding of translationally-interlocked configurations is thus comparable to planarisation, which is a task handled by available solvers, like [42] or [40]. We notice that finding interlocked solutions for quadrilateral meshes is approximately as difficult as planarising a hexagonal mesh.

Second, it is possible to consider the orientation as fixed and to consider the reference mesh as a design variable. It should be noted that equation (4) is a function of the normals of the edges and (implicitly) of the edge orientation. Therefore, any geometrical transformation mapping a mesh to another mesh without changing the edge orientation leaves the quantities in equation (4) invariant. The interlocking property is thus invariant by isometries (translations, rotations) but also by discrete parallel transformations, which map edges to parallel edges. This geometrical transformation is at the core of the study of discrete offsets [43]. The ensemble of discrete parallel transformations is a linear space, which can be determined by using classical methods in linear algebra, like Singular Value Decomposition [43]. A lower-bound for the dimension of the design space has been proposed in [43], and this lower-bound has been estimated for a collection of meshes typically employed in architecture in [44]. For a quadrilateral mesh with N facets, the dimension of this design space is proportional to $\sqrt{N}$. The dimensionality of the design space also increases for hexagonal meshes, which is in accordance with the previous remark.

Remarkably, discrete parallel transformations also appear in structural analysis applied to masonry structures, as they play a particular role in graphic statics [45, 46]. Indeed, a discrete parallel transformation of a force diagram leaves the form diagram unchanged and corresponds thus to a geometrical interpretation of a state of self-stress. In topologically interlocked masonries, the discrete parallel transformations come from a dual perspective, since the necessary condition for interlocking was derived from a kinematic condition and not an equilibrium one.

A necessary and sufficient condition to generate topologically interlocked masonry has been introduced for structures generated from quadrilateral meshes. It has been extended to other meshes and a simple topological operation has been proposed to provide topological interlocking for structures with free-edges. The quadrilateral mesh being the basis for these extensions, it is studied in more detail in the followings of this article.

7. Some examples and validations of the criteria

In this part some applications of this criteria are produced to validate the method and highlight its efficiency. A discussion on practical implementation is provided.

7.1. Planar quadrangle

Even if system (3) is also valid for blocks derived from non planar quadrangle, realistic and interesting applications concern rather planar quadrangle. Let us consider a planar quadrangle (a face of a PQ mesh) and the notation introduced in Fig. 5. The inequalities (i), (ii) and (iii) can thus be rewritten in terms of $\{\alpha_1, \alpha_2, \alpha_3, \alpha_4\}$ and edges unit direction vectors $\{\vec{t}_1, \vec{t}_2, \vec{t}_3, \vec{t}_4\}$. Hence the set of inequalities becomes (5), which is easier to handle.

$$\begin{aligned}
&[\tan\alpha_3 \sin\omega_{12} + \tan\alpha_2 \sin\omega_{31} + \tan\alpha_1 \sin\omega_{23}] \\
&\quad \cdot [\tan\alpha_4 \sin\omega_{12} + \tan\alpha_2 \sin\omega_{41} + \tan\alpha_1 \sin\omega_{24}] < 0 \\
\text{and}\quad &[\tan\alpha_3 \sin\omega_{12} + \tan\alpha_2 \sin\omega_{31} + \tan\alpha_1 \sin\omega_{23}] \\
&\quad \cdot [\tan\alpha_3 \sin\omega_{42} + \tan\alpha_2 \sin\omega_{34} + \tan\alpha_4 \sin\omega_{23}] < 0 \\
\text{and}\quad &[\tan\alpha_3 \sin\omega_{12} + \tan\alpha_2 \sin\omega_{31} + \tan\alpha_1 \sin\omega_{23}] \\
&\quad \cdot [\tan\alpha_1 \sin\omega_{43} + \tan\alpha_3 \sin\omega_{14} + \tan\alpha_4 \sin\omega_{31}] < 0
\end{aligned} \tag{5}$$

The numbers ω_{ij} are defined as $\omega_{ij} = \left(\widehat{\vec{t}_i, \vec{t}_j}\right)$. They depend only on the geometry of the input mesh and can be considered as design input in a typical workflow where one would calibrate the shape to specific needs (fabrication, statics, etc.) and where the stereotomy would be chosen afterwards. In such a workflow, the values $\sin\omega_{ij}$ would be treated as constants, and α_i would be the only design parameters. Equation (5) clearly illustrates the non-linearity of equation (3) in α, but it is a set of quadratic inequations in $\tan\alpha_i$, which hints that the tangents of the angles could be used as variables in a quadratic programming algorithm. Some specific cases admit closed form solution, like for meshes constructed on surfaces of translation.

7.2. Implementation of the criterion

By taking $\beta_i = \tan\alpha_i$ as design variables, and writing $s_{ij} = \sin\omega_{ij}$, equation (5) becomes a quadratic inequality. Following classical numerical methods [42], we can introduce dummy variables $\mu_{i,b}$ for each block b and turn inequalities into equalities.

$$\begin{aligned}
&[\beta_3 s_{12} + \beta_2 s_{31} + \beta_1 s_{23}] \cdot [\beta_4 s_{12} + \beta_2 s_{41} + \beta_1 s_{24}] + \mu_1^2 = 0 \\
&[\beta_3 s_{12} + \beta_2 s_{31} + \beta_1 s_{23}] \cdot [\beta_3 s_{42} + \beta_2 s_{34} + \beta_4 s_{23}] + \mu_2^2 = 0 \\
&[\beta_3 s_{12} + \beta_2 s_{31} + \beta_1 s_{23}] \cdot [\beta_1 s_{43} + \beta_3 s_{14} + \beta_4 s_{31}] + \mu_3^2 = 0
\end{aligned}$$

This quadratic constraint can be treated with an iterative method, like a guided projection algorithm introduced in [42]. This algorithm uses a linearisation of quadratic constraints, which is an easy procedure, and minimises an objective function. The dimension of the design space as well as formulation of constraints is comparable to those described in [42], so that similar performance is expected. The inequality and equalities derived in this article can thus be employed in a structural or geometrical optimisation procedure as an interlocking constraint. Objective functions, like load factor maximisation under a given load case, could be optimised.

The inequality constraints presented in this article is not symmetrical, as it chooses a set of normals $\vec{n_1}, \vec{n_2}, \vec{n_3}$ and assumes that they are not co-planar. In practice, the constraints can be duplicated 3 times for a quadrilateral facet to make the problem independent of such a choice. Those constraints will be redundant in many cases and thus increase computational time, but this duplication significantly improves the stability of optimisation procedures.

7.3. Surfaces of translation

The first free-form surfaces covered with planar quadrilaterals were translation surfaces [47]. They are generated by translating a curve along another curve, and are thus covered with planar parallelograms. Eq. 5 can be simplified when the planar quadrangle is a parallelogram (Fig. 12). Indeed, opposite angles have the same values:

$$\begin{aligned} \omega_{12} &= \omega_{34} \\ \omega_{23} &= \omega_{41} \end{aligned}$$

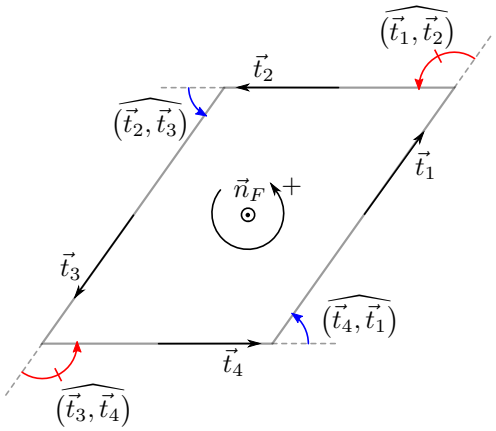

Figure 12: Parallelogram

Moreover, consecutive angles are supplementary:

$$\begin{aligned} \omega_{12} + \omega_{23} &= \pi \\ \omega_{34} + \omega_{41} &= \pi \end{aligned}$$

Hence the following relations:

$$\begin{cases} \sin\omega_{12} = \sin\omega_{23} = \sin\omega_{34} = \sin\omega_{41} \\ \sin\omega_{13} = \sin\omega_{24} = 0 \end{cases}$$

The right member of Eq. 5 then becomes:

$$\begin{cases} \sin^2\omega_{12}\,(\tan\alpha_3 + \tan\alpha_1)\,(\tan\alpha_4 + \tan\alpha_2) < 0 \\ \sin^2\omega_{12}\,(\tan\alpha_3 + \tan\alpha_1)\,(\tan\alpha_2 + \tan\alpha_4) < 0 \\ \sin^2\omega_{12}\,(\tan\alpha_3 + \tan\alpha_1)\,(-\tan\alpha_1 - \tan\alpha_3) < 0 \end{cases}$$

Since $\cos\alpha_1 \cos\alpha_2 \cos\alpha_3 \cos\alpha_4$ is positive, multiplying the inequalities by this value does not change their sign. Hence, using the trigonometry formula:

$$(\tan A + \tan B) \cdot \cos A \cdot \cos B = \sin(A + B)$$

the necessary and sufficient condition for a block generated from a parallelogram reads thus as follows:

$$\sin(\alpha_1 + \alpha_3) \cdot \sin(\alpha_2 + \alpha_4) < 0 \tag{6}$$

This equation can be further simplified, since:

$$\begin{cases} -2\pi < \alpha_1 + \alpha_3 < 0 \\ 0 < \alpha_2 + \alpha_4 < 2\pi \end{cases} \tag{7}$$

or

$$\begin{cases} 0 < \alpha_1 + \alpha_3 < 2\pi \\ -2\pi < \alpha_2 + \alpha_4 < 0 \end{cases} \tag{8}$$

Therefore, the interlocking condition is linear in α_i for parallelograms due to remarkable trigonometric identities. The domain of admissible values for $(\alpha_1, \alpha_2, \alpha_3, \alpha_4)$ is thus a set of half planes. If one select one of the half hyperplanes of $\mathbb{R}^4$, for example by setting the sign of α_1 and α_2, there is one half hyperplane of admissible solutions for equations (7) and (8). Result (6) is actually the demonstration of the assertion written in the section-**??**, the block generated from a parallelogram planar mesh is translationally interlocked. This result can be applied to the generation of topologically interlocked masonries on surfaces of translations.

7.4. Other examples

If the sign of the four angles α_1, α_2, α_3 and α_4 ($0° < |\alpha_i| < 90°$) alternate between positive and negative values, meaning $(\alpha_i \cdot \alpha_{i+1}) < 0$, then,

$$\sin(\alpha_1 + \alpha_3) \cdot \sin(\alpha_2 + \alpha_4) = -\sin(|\alpha_1| + |\alpha_3|) \cdot \sin(|\alpha_2| + |\alpha_4|) < 0 \tag{9}$$

Hence, Eq. 6 is verified and a general result is that *a block generated from a parallelogram quadrangle with angles α_i whose signs alternate between positive and negative is translationally interlocked.*

This proves the known result that the assembly of tetrahedrons (generated from a mesh of squares with

alternated angles) is indeed translationally interlocked.

Moreover, Eq. 6 allows to generate translationally interlocked assemblies from a mesh of paralellograms with angles whose sign is not necessarily alternated. For example, using a mesh of squares and $\alpha_1 = 60°$, $\alpha_2 = 30°$, $\alpha_3 = -30°$ et $\alpha_4 = -60°$, the inequality of Eq. 6 is satisfied. The signs of the angles α_i do not successively alternate between positive and negative but the assembly is translationally interlocked.

Another interesting result is that it can be easely demonstrated that for non regular quadrangular mesh the interlocking property is not always effective satisfied. Indeed, consider the two assemblies illustrated Fig. 13.Let α_1, α_2, α_3 and α_4 be four angles whose signs alternate between positive and negative ($\alpha_i \cdot \alpha_{i+1} < 0$ pour $i \in \mathbb{Z}/4\mathbb{Z}$). The first one is generated from a mesh of squares, the other one from an irregular mesh whose center face is a trapezoid. For both assemblies, the same angles $\alpha_1 = -15°$, $\alpha_2 = 45°$, $\alpha_3 = -15°$ and $\alpha_4 = 45°$ are used for the planes inclination of the center block. The signs of these angles alternate between negative and positive. According to the previous corollary, the first assembly is translationally interlocked. On the other hand, the second assembly is not interlocked. Indeed, for the middle quadrangle:

$$\begin{aligned}\omega_{12} &= 110°\\ \omega_{23} &= 110°\\ \omega_{34} &= 70°\\ \omega_{41} &= 70°\end{aligned}$$

It can easily be verified that none of the left-hand terms in equation 5 is negative. The block generated from the middle quadrangle is therefore not translationally interlocked. There exists at least one translation to take the block out of the assembly without colliding its neighbours. Such a displacement is illustrated on Fig. 13c.

8. Applications and prototypes

The geometrical condition for topological interlocking derived in the previous sections assumes a perfect planar contact. In reality, some imperfections might change the nature of the contacts between blocks and cancel out the interlocking behaviour. Since modelling of such imperfections is a difficult task, the preferred method is to construct small physical models using rapid prototyping or digital fabrication techniques. The aim of this section is thus to present physical models that explore the potential of topologically interlocked masonries on curved shapes and to discuss the influence of technology, fabrication process and tolerance on the feasability of their assembly. Several applications of interlocked masonries were designed and studied following the rules established before. Two case studies are presented here, one of the two prototypes has been built without formwork.

8.1. Double curvature vault

In this first application, the geometry is a moulding surface with positive gaussian curvature (Fig. 14), obtained by sweeping the blue plane curve (*génératrice*) along another plane curve (*rail*), here chosen as a catenary. This geometrical strategy yields a PQ-mesh, and even a conical mesh [48], the resultating shape has a high structural efficiency.

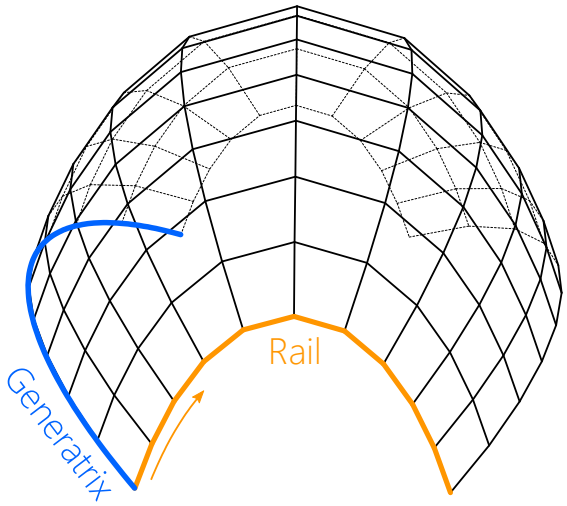

Figure 14: PQ mesh in a double positive curvature surface

A topological interlocking systems was obtained by the new *moving cross-section* procedure. The system (3) is verified for each block, and after truncation operation, the following structure is obtained Fig. 15. A mock-up was printed in ABS, the element variety can be observed on fig. 16. The boundaries are not topologically interlocked, since the boundary blocks only have three neighbours. This was dealt with by constructing a monolithic boundary, a choice that is well suited for the model scale (length of 25cm), but not for the architectural scale. Although theoretically topologically interlocked, the model was sensitive to tolerance of assembly and production: a slight error of assembly resulting in edge/face rather that face/face contacts. However, the funicularity of the vault created a natural locking along the vertical direction. The need to accomodate tolerances is thus crucial in the construction of topologically interlocked masonries. One may thus understand why digital fabrication and robotics are needed to realise such structures. It should however be mentioned that the small block dimensions makes them relatively more sensitive to an error of assembly than larger blocks, like the ones that were used for the second case-study.

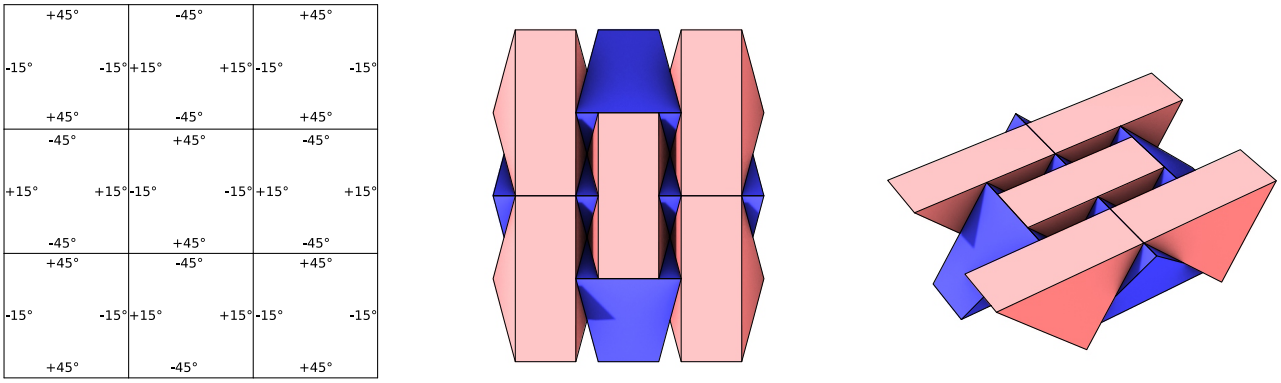

(a) Assembly generated for a regular squares lattice. Values on the edge of the mesh illustrated at lef are the value of α_i. For each block, the signs of the angles α_1, α_2, α_3 and α_4 α_i successively alternate between positive and negative. The assembly is translationally interlocked.

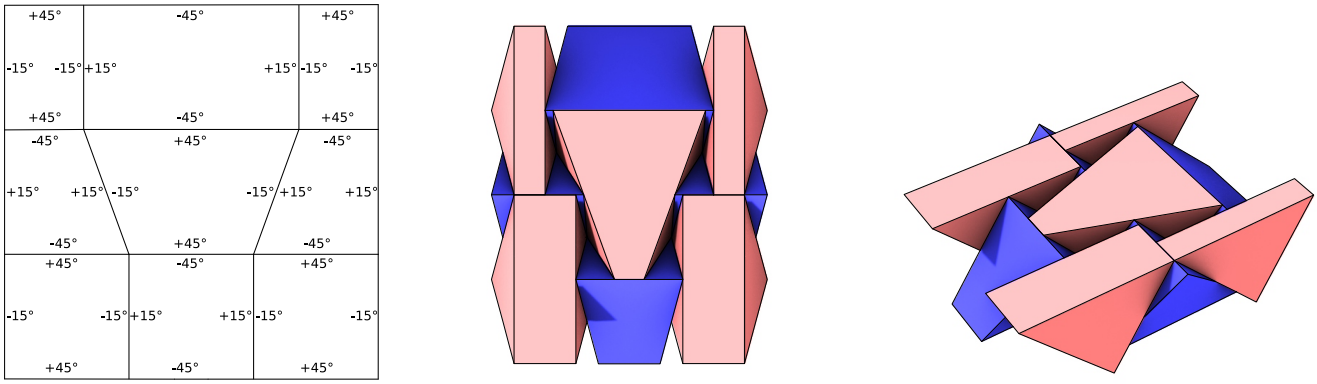

(b) Assembly on a non regular lattice. The middle quadrangle is a trapezoid. Angles α_i have the same values as (a)but the assembly is not translationally interlocked.

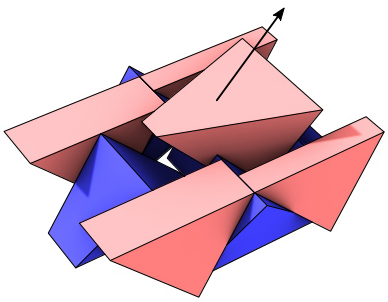

(c) The block generated from the trapezoid is not translationally locked. The arrow represents a motion to take it out of the subset without colliding with its neighbours.

Figure 13: Different meshes, with different α_i (signs alternate between positive and negative). The first assembly is translationally interlocked but not the second one.

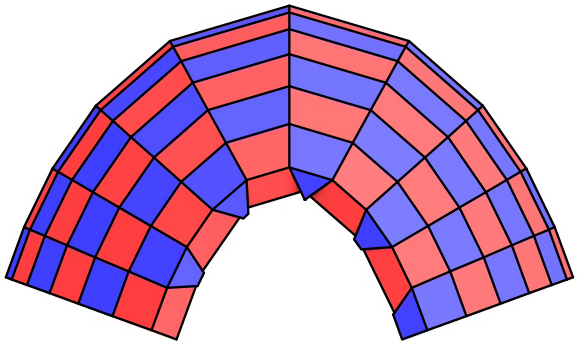

(a) front view

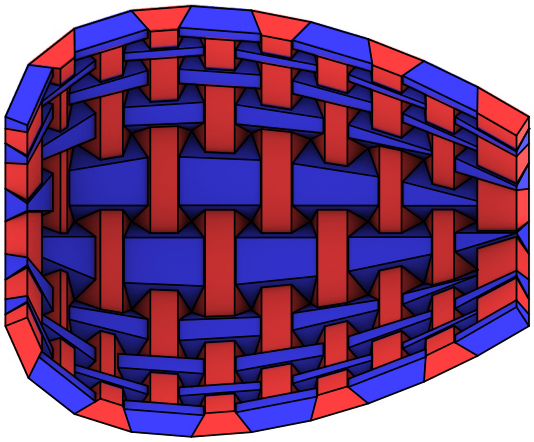

(b) from below

Figure 15: A topologically interlocking vault

8.2. Corolla

This second application, is a negatively curved surface (fig.17), inspired by the Byzantines systems as each horizontal hoop might *grip* the next one. Actually it exists tension loading in these hoops, and it is interesting to try an interlocked solution in such a difficult case study. This surface is a surface of revolution and can thus easily be meshed by planar quadrangles.

Several discretization may be proposed, concerning for example the angle of the joint planes. If they are normal to the surface as on the left figure 18, the resulting structure is unstable, since nothing is able to bear tensile stresses in horizontal hoops due to the self-weight of the structure. By tilting the joints as on the right Figure 18, a topological interlocked solutions is given, meaning that each block and group of blocks are geometrically locked and verify equation 3. But is it stable, buildable, and able to support loading and consequently an interesting architectural solution? This paper doesn't pretend to be able to answer theoretically and definitely to this question, more developments would be needed, however, finite-element and mock-up may will help to investigate this challenge.

The structure, which consists of 80 blocks is chosen as axisymetric, and reduced to 10 different blocks. An elementary slice is described on figure 19.

The structure is stable if each block is held by is neighbours. The idea is to design the blocks so that each new block is supported by the three planar contacts with the blocks below and on each sides. The moment equilibrium of the block during assembly needs to be fulfilled: the position of the center of gravity of the block with respect to the points of contact should thus carefuly be chosen: it may help if the center of gravity of the new block is above the lower block and not above the void. The design of the blocks verifies this requirement. These blocks could nevertheless slide, but the sliding is prevented by its neighbours below on each side. Once half of the blocks of the circle are put in place, the missing blocks can be added. Once the hoop is completed, the prior hoop becomes topologically interlocked, so that the stability condition for the cantilevering has to be satisfied only for the outer hoop. Figure (20) shows a step by step animation of the technique.

Following this principle, and to identify stable and interesting geometries and tilt angles, an iterative process (trial and error) was made, involving mock-ups and a finite element approach.
Abaqus/Explicit software was used, each block is meshed by C3D3 tetrahedral linear elements. A Coulomb friction and *hard contact* for normal interaction (non interpenetration), are introduced between blocks. A convergence analysis was conducted and the necessary number of element is of 60000 elements per block, due to the corner and angle singularities. A discrete element method (DEM) could be used for more efficient calculations (considering each block as rigid, only one element per block) but not proposed in this paper. For calculations and material data, classical mortar and 30° Coulomb friction are considered. Concerning boundary conditions, the interface between the ground and the blocks of the first hoop is rigid. The diameter of the first and fifth hoop is respectively 30 cm and 90 cm. Only the weight load is considered.
For the precise geometry on the Fig.20, the explicit scheme calculation converges without instabilities, and without exceeding the maximum strength value of the material (located in the corners of blocks, which are the weak points), and provided a good reason to believe that a prototype would actually work.
The prototype was made with 3d printed blocks (a mix of resin and sand), is 90 cm wide and was realised without any formwork (Fig.21). The outer hoop is not topologically interlocked, since there are only three planar con-

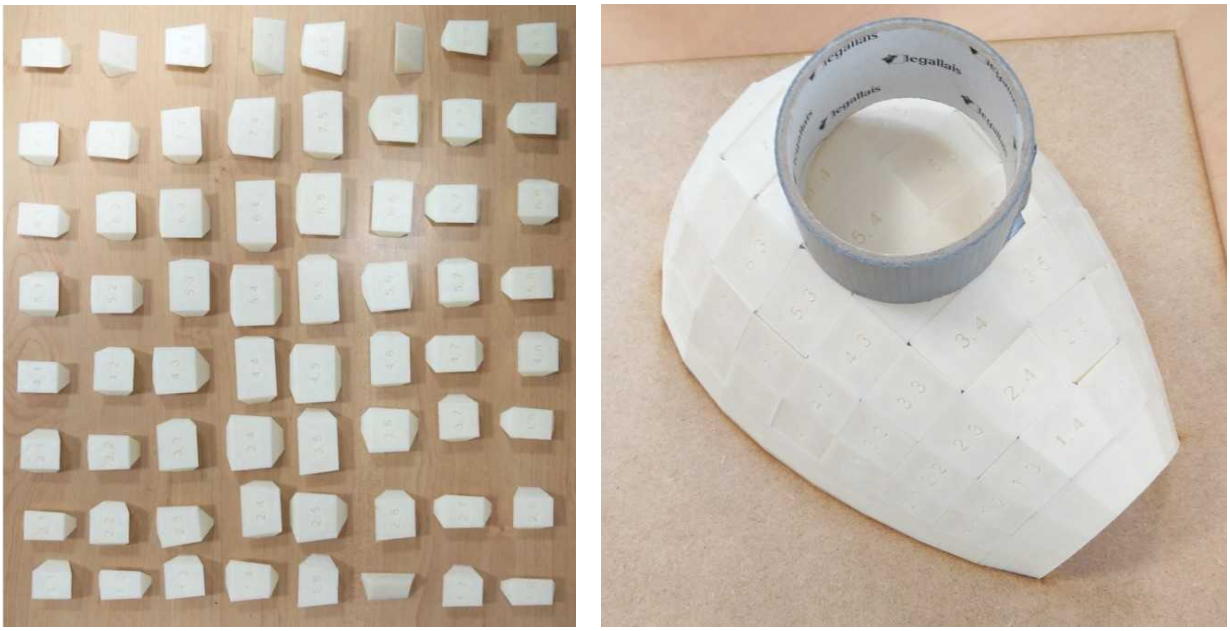

Figure 16: Mock-up and the set of blocks

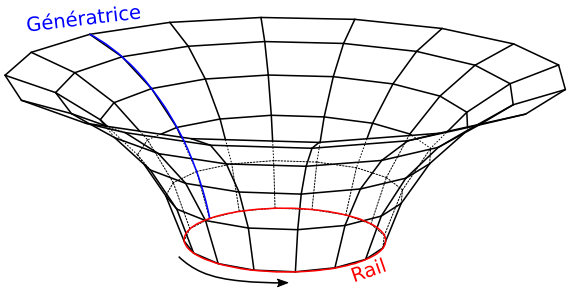

Figure 17: The corolla and the planar quadrangular meshing

tacts per block. A possible improvement to circumvent this structural weakness would be to add a pre-stress cable that locks the outer hoop in compression, or to use different blocks, as suggested in Section 5.

8.3. Discussion on construction and fabrication

The two prototypes allowed to identify some peculiarities in the construction of topologically interlocked masonries. First, the relatively small scale of the prototypes makes them quite sensitive to tolerance of assembly. The precision of manual assembly relative (in the millimetric range) to block dimension (approximately 10cm) is not enough to guarantee planar contacts between the block faces, so that some edge/face contacts exist in the two prototypes. The precision can be improved with guiding protusions in the blocks that are aligned with the cone of assembly, and this approach has been chosen for the second case-study. Nonetheless, we were able to construct a masonry with a tension hoop without formwork, which demonstrates the practical interest of the method and of topologically interlocked masonries. In a context of digital fabrication and assembly, and at a building scale with blocks in the metric range, a better relative precision could be achieved, but this requires to compensate errors of assembly on the fly, a relatively intuitive task performed by humans, but a computationally involved task for a robotic assembly system.

9. Conclusions

The context of the work concerns the development of robotics in construction and the focus here is made on complex masonry structures, as the new development of the digital tools, for design and construction, may help for new challenges and solutions. The paper presents new results about topological interlocking sytems and some possibilities they present to build without formwork as construction without the use of formwork may be an important issue in relation to both productivity increasing and decreasing of waste generated on a construction site. The design of this kind of masonry is standard for planar structures, and in this paper a generalization is proposed for the design of curved structures, in a parametric and generative design context.

First a state of the art concerning the topologically self-locking assemblies and some of their properties is presented, the way special design may provide bending stiffness and ductile behaviour – even if the material is fragile.

Then, an existing procedure devoted to the design of topologically interlocking masonries (limited to plane geometries, regular meshes and rectangular elements) is generalized to the design of curved structures, meshed by plane quadrangles. The quadrangles are no more

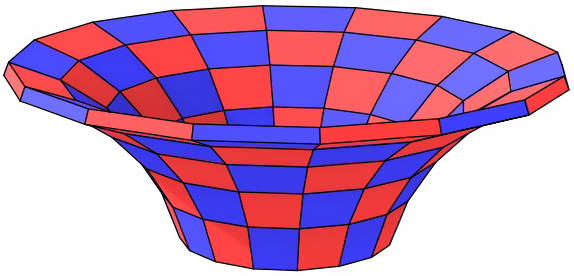

(a) Normal joint planes

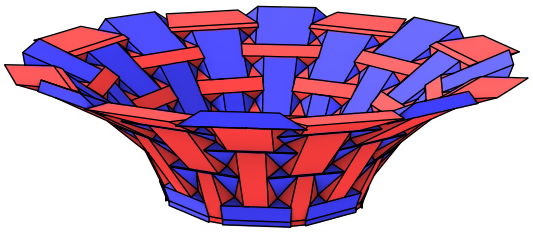

(b) A topological interlocked solution

Figure 18: Two different discretization, and one topological interlocked solution

necessarily regular, and a criteria is proposed to check the topological blocking in translation of the elements. An extension to non-quadrangular meshes is also proposed, and the invariance under mesh parallelism transformations is highlighted. The blocking in rotation was not studied here but it would be interesting to try to find similar conditions for the rotation locking.

Thanks to the numerical workflow, generative design and criteria checking, two specific prototypes are investigated and built. The first one is a vault, and the second one a corolla with negative double curvature. For this second application it exists tension loading in the horizontal hoops, and an interlocked solution has to bear these stresses both from a geometrical and mechanical point of view. The workflow permits to propose a geometrical solution, providing shapes of the blocks and joint angles. To ensure a mechanical stability of the final structure, a finite element modeling of the corolla was made with Abaqus/Explicit software. Only the weight load is considered, and a stable solution is obtained, with no exceeding the maximum strength value of the material. This first mechanical assessment, provides a good reason to believe that the concept will work and a prototype with a 90 cm diameter was realised. Made with 3d printed blocks (a mix of resin and sand), it is erected without any formwork. The finite element simulation doesn't simulate yet the mounting process but only the final structure. It has to be done if the need is to know if the masonry needs formworks or not.

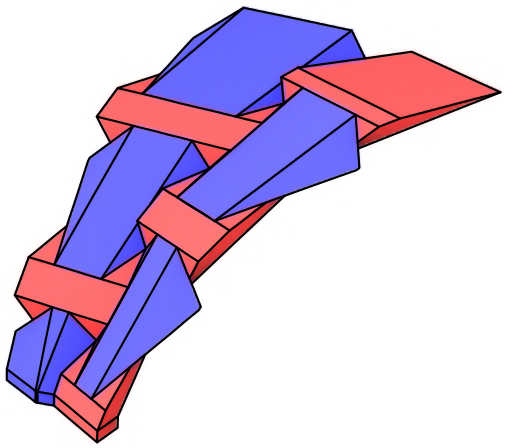

Figure 19: A typical slice of the corolla, 10 different blocks. 8 slices for the whole corolla

Future work should study more precisely the structural behaviour of topologically interlocked masonries. Previous works on topologically interlocked materials show that translational interlocking seems to guarantee structural ductility even with brittle material. This should be confirmed with more refined studies for the various load cases at stake at the architectural scale.

Concerning the perspectives of the study and the aim relative to a global digital workflow for new and innovative masonries, as introduced in the introduction, some developments are in progress to permit a robotic manipulation of the blocks including the autonomous recognition and managment of the complex shapes thanks to vision and Convolutional Neural Network ([4]). A real demonstrator integrating an ABB IRB 120 arm, parallelepipedic blocks and three lowcost webcams was set up to demonstrate the feasibility of the method building a curved wall using parallelepipedic bricks, as shown in the figure 22.

Aknowledgment

This work was carried out in the framework of a PhD Thesis on digital fabrication. The authors gratefuly aknowledge the funding from Ecole des Ponts ParisTech and Build'in, a plateform of its Co-Innovation Lab.

References

[1] F. Barbosa, J. Woetzel, J. Mischke, M. Ribeirinho, M. Sridhar, M. Parsons, N. Bertram, S. Brown, Reinventing construction: A route to higher productivity, Executive summary, McKinsey

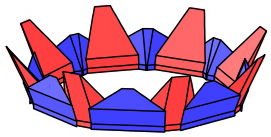

(a) first hoop

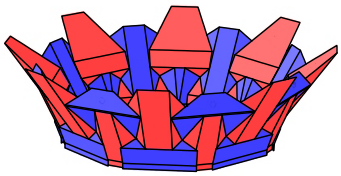

(b) second hoop

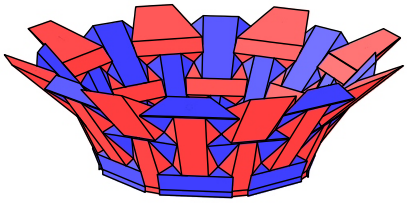

(c) third hoop

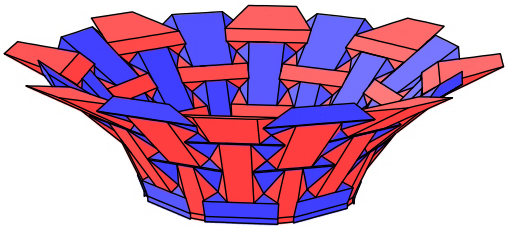

(d) fourth hoop

Figure 20: Step by step erection of the corolla

Global Institute, last accessed on 20/01/20 (feb 2017). URL https://www.mckinsey.com/industries/capital-projects-and-infrastructure/our-insights/reinventing-construction-through-a-productivity-revolution

[2] T. Bock, S. Langenberg, Changing building sites: Industri-

(a)

(b)

(c)

(d)

Figure 21: Corolla in construction. The wood square basement is 60 cm long.

alisation and automation of the building process, Architectural Design 84 (3) (2014) 88–99, last accessed 20/01/20. doi:10.1002/ad.1762.
URL https://onlinelibrary.wiley.com/doi/abs/10.1002/ad.1762

[3] T. Bonwetsch, D. Kobel, F. Gramazio, M. Kohler, The informed wall: Applying additive digital fabrication techniques on architecture, in: Synthetic Landscapes - ACADIA 2006 International Conference, 2006, pp. 489–495.
URL https://www.scopus.com/inward/record.uri?eid=2-s2.0-79955473966&partnerID=40&md5=13c2047c2491700b04d6b5e0110a8236

[4] V. Loing, R. Marlet, M. Aubry, Virtual training for a real application: Accurate object-robot relative localization without calibration, International Journal of Computer Vision 126 (9) (2018) 1045–1060. doi:10.1007/s11263-018-1102-6.
URL https://doi.org/10.1007/s11263-018-1102-6

[5] Monitoring of solid waste in hong kong: Waste statistics for 2013, Executive summary, Environmental Protection Department (feb 2015).
URL https://www.wastereduction.gov.hk/sites/default/files/msw2013.pdf

[6] D. W. Johnston, Design and construction of concrete formwork, in: E. G. Nawy (Ed.), Concrete Construction Engineering Handbook, CRC Press, Boca Raton, 2008, pp. 7–1–7–49, ISBN: 9780849374920.

[7] A. Choisy, L'art de bâtir chez les Byzantins (the art of building among the Byzantines), Librairie de la Société anonyme de publications périodiques, 1883, ISBN: 9788827119112.

[8] M. Deuss, D. Panozzo, E. Whiting, Y. Liu, P. Block, O. Sorkine-Hornung, M. Pauly, Assembling self-supporting structures, ACM Transactions on Graphics 33 (6) (2014) 1. doi:10.1145/2661229.2661266.

[9] G. T. C. Kao, A. Körner, D. Sonntag, L. Nguyen, A. Menges, J. Knippers, Assembly-aware design of masonry shell structures: a computational approach, in: Proceedings of the IASS Annual Symposium 2017, Hamburg, 2017, last accessed on 20/01/20.
URL https://www.researchgate.net/publication/320188621_Assembly-aware_design_of_masonry_shell_structures_a_computational_approach

[10] A. V. Dyskin, Y. Estrin, A. J. Kanel-belov, E. Pasternak, Toughening by fragmentation - how topology helps, Advanced Engineering Materials 3 (11) (2001) 885–888. doi:10.1002/1527-2648(200111)3:11<885::AID-ADEM885>3.0.CO;2-P.

[11] M. F. Ashby, Y. J. M. Bréchet, Designing hybrid materials, Acta Materialia 51 (19) (2003) 5801–5821. arXiv:arXiv:1011.1669v3, doi:10.1016/S1359-6454(03)00441-5.

[12] A. V. Dyskin, Y. Estrin, A. J. Kanel-Belov, E. Pasternak, A new concept in design of materials and structures: Assemblies of interlocked tetrahedron-shaped elements, Scripta Materialia 44 (12) (2001) 2689–2694. doi:10.1016/S1359-6462(01)00968-X.

[13] A. V. Dyskin, Y. Estrin, E. Pasternak, H. C. Khor, A. Kanel-Belov, Fracture resistant structures based on topological interlocking with non-planar contacts, Advanced Engineering Materials 5 (3) (2003) 116–119. doi:10.1002/adem.200390016.

[14] Y. Estrin, A. V. Dyskin, E. Pasternak, S. Schaare, S. Stanchits, A. J. Kanel-Belov, Negative stiffness of a layer with topologically interlocked elements, Scripta Materialia 50 (2) (2004) 291–294. doi:10.1016/j.scriptamat.2003.09.053.

[15] A. Autruffe, F. Pelloux, C. Brugger, P. Duval, Y. Bréchet, M. Fivel, Indentation behaviour of interlocked structures made of ice: Influence of the friction coefficient, Advanced Engineering Materials 9 (8) (2007) 664–666. doi:10.1002/adem.200700111.

[16] C. Brugger, Y. Bréchet, M. Fivel, Experiments and Numerical Simulations of Interlocked Materials, Advanced Materials Research 47-50 (2008) 125–128. doi:10.4028/www.scientific.net/AMR.47-50.125.
URL http://www.scientific.net/AMR.47-50.125

[17] S. Khandelwal, T. Siegmund, R. Cipra, J. Bolton, Transverse loading of cellular topologically interlocked materials, International Journal of Solids and Structures 49 (18) (2012) 2394 – 2403. doi:https://doi.org/10.1016/j.ijsolstr.2012.04.035.
URL http://www.sciencedirect.com/science/article/pii/S0020768312001886

[18] M. Dugué, Experiments and simulations of interlocked materials, Ph.D. thesis, Université de Grenoble, last accessed on 20/01/20 (2013).
URL https://tel.archives-ouvertes.fr/tel-00820069

[19] A. F. Frézier, La théorie et la pratique de la coupe des pierres et des bois, pour la construction des voûtes et autres parties des bâtiments civils et militaires, ou Traité de stéréotomie à l'usage

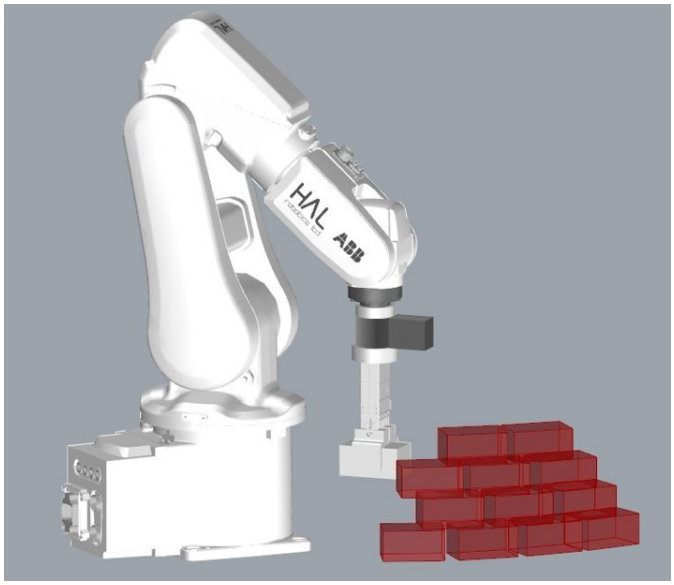

(a) Digital design of a slightly curved wall. The toolpath was generated using HAL Robotics software (https://hal-robotics.com/).

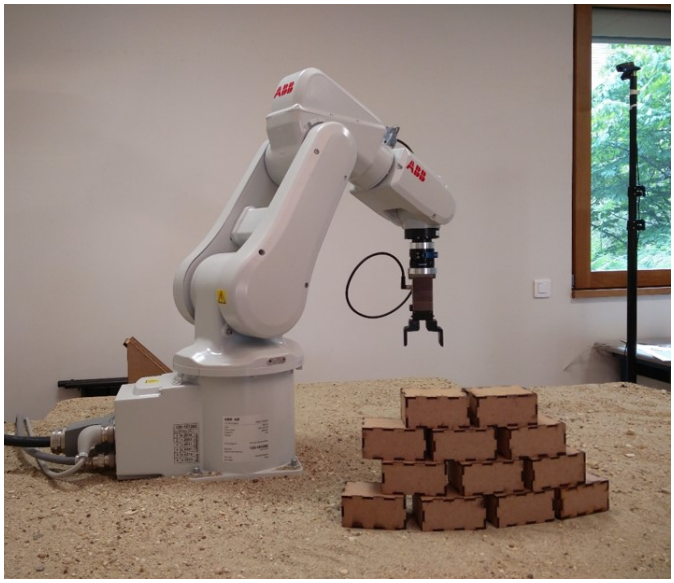

(b) Wall built using artificial vision algorithm for block location and placement estimation

Figure 22: Design and robotic fabrication of a wall https://youtu.be/-oXSPiymryg

de l'architecture (The theory and practice of stone cutting and woods, for the construction of the vaults and other parts of the civilian and military buildings), Jombert, C. A., 1737, ISBN: 978-1293894729.

[20] A. V. Dyskin, Y. Estrin, A. Kanel-Belov, E. Pasternak, Topological interlocking of platonic solids: A way to new materials and structures, Philosophical Magazine Letters 83 (3) (2003) 197–203. doi:10.1080/0950083031000065226.

[21] M. Glickman, The G-Block System of Vertically Interlocking Paving, in: Second International Conference on Concrete Block Paving, 1984, pp. 1–4, last accessed on 20/01/20.
URL http://www.sept.org/techpapers/361.pdf

[22] Y. Feng, T. Siegmund, E. Habtour, J. Riddick, Impact mechanics of topologically interlocked material assemblies, International Journal of Impact Engineering 75 (2015) 140–149. doi:10.1016/j.ijimpeng.2014.08.003.
URL http://dx.doi.org/10.1016/j.ijimpeng.2014.08.003

[23] H. T. D. Yong, Utilisation of topologically-interlocking osteomorphic blocks for multi-purpose civil construction, Ph.D. thesis, The University of Western Australia, last accessed: 20/01/20 (2011).
URL https://research-repository.uwa.edu.au/en/publications/utilisation-of-topologically-interlocking-osteomorphic-blocks-for-m

[24] F. Fleury, Evaluation of the Perpendicular Flat Vault Inventor' s Intuitions through Large Scale Instrumented Testing, in: Third International Congress on Construction History, 2009.

[25] M. Brocato, L. Mondardini, Geometric methods and computational mechanics for the design of stone domes based on Abeille's bond, in: Advances in Architectural Geometry 2010, Vol. 1, Springer Vienna, Vienna, 2010, pp. 149–162, iSBN: 9783709103081. arXiv:arXiv:1011.1669v3, doi:10.1007/978-3-7091-0309-8_11.
URL http://link.springer.com/10.1007/978-3-7091-0309-8{_}11

[26] M. Brocato, W. Deleporte, L. Mondardini, J.-E. Tanguy, A Proposal for a New Type of Prefabricated Stone Wall, International Journal of Space Structures 29 (2) (2014) 97–112. doi:10.1260/0266-3511.29.2.97.
URL http://journals.sagepub.com/doi/10.1260/0266-3511.29.2.97

[27] G. Fallacara, Digital stereotomy and topological transformations: reasoning about shape building, in: Proceedings of the Second International Congress on Construction History [Volume 1], 2006, pp. 1075–1092, ISBN: 0701702036.
URL http://www.arct.cam.ac.uk/Downloads/ichs/vol-1-1075-1092-fallacara.pdf

[28] A. J. Kanel-Belov, A. V. Dyskin, Y. Estrin, E. Pasternak, I. A. Ivanov-Pogodaev, Interlocking of convex polyhedra: Towards a geometric theory of fragmented solids, Moscow Mathematical Journal 10 (2) (2010) 337–342. doi:https://doi.org/10.17323/1609-4514-2010-10-2-337-342.

[29] I. M. Vella, T. Kotnik, Geometric Versatility of Abeille Vault, in: Proceedings of the 34th International Conference on Education and Research in Computer Aided Architectural Design in Europe, Oulu, Finland, 24.-26, Vol. 2, 2016, pp. 391–397.
URL http://papers.cumincad.org/cgi-bin/works/Show?_id=ecaade2016_011&sort=DEFAULT&search=kotnik&hits=7

[30] M. Weizmann, O. Amir, Y. J. Grobman, Topological interlocking in buildings: A case for the design and construction of floors, Automation in Construction (2016). doi:10.1016/j.autcon.2016.05.014.

[31] J. Salençon, Calcul à la rupture et analyse limite, Presses de l'école nationale des Ponts et Chaussées (Yield design and limit analysis), 1983, iSBN: 2859780599.

[32] Z. Wang, P. Song, F. Isvoranu, M. Pauly, Design and structural optimization of topological interlocking assemblies, ACM Trans. Graph. 38 (6) (Nov. 2019). doi:10.1145/3355089.3356489.
URL https://doi.org/10.1145/3355089.3356489

[33] J. Glymph, D. Shelden, C. Ceccato, J. Mussel, H. Schober, A parametric strategy for free-form glass structures using quadrilateral planar facets, Automation in construction 13 (2) (2004) 187–202. doi:https://doi.org/10.1016/j.autcon.2003.09.008.

[34] Y. Liu, H. Pottmann, J. Wallner, Y.-L. Yang, W. Wang, Geometric modeling with conical meshes and developable surfaces, ACM Trans. Graph. 25 (3) (2006) 681–689. doi:10.1145/1141911.1141941.
URL https://doi.org/10.1145/1141911.1141941

[35] R. Mesnil, C. Douthe, O. Baverel, B. Léger, Marionette meshes: modelling free-form architecture with planar facets, International Journal of Space Structures 32 (3-4) (2017) 184–198. doi:https://doi.org/10.1177/0266351117738379.

[36] I. M. Vella, T. Kotnik, Stereotomy, an early example of a material system, in: ShoCK! - Sharing Computational Knowledge!, Volume 2, 2017, last accessed: 20/01/20.
URL https://www.researchgate.net/publication/319941904

[37] R. Mesnil, C. Douthe, O. Baverel, T. Gobin, Form finding of nexorades using the translations method, Automation in Construction 95 (2018) 142–154. doi:https://doi.org/10.1016/j.autcon.2018.08.010.

[38] R. Mesnil, C. Douthe, O. Baverel, B. Leger, Generalised cyclidic nets for shape modelling in architecture, International Journal of Architectural Computing 15 (2) (2017) 148–168. doi:https://doi.org/10.1177/1478077117714917.

[39] R. Mesnil, C. Douthe, O. Baverel, B. Léger, Morphogenesis of surfaces with planar lines of curvature and application to architectural design, Automation in Construction 95 (2018) 129–141. doi:https://doi.org/10.1016/j.autcon.2018.08.007.

[40] S. Bouaziz, M. Deuss, Y. Schwartzburg, T. Weise, M. Pauly, Shape-up: Shaping discrete geometry with projections, Comput. Graph. Forum 31 (5) (2012) 1657–1667. doi:10.1111/j.1467-8659.2012.03171.x.
URL https://doi.org/10.1111/j.1467-8659.2012.03171.x

[41] B. Deng, S. Bouaziz, M. Deuss, J. Zhang, Y. Schwartzburg, M. Pauly, Exploring local modifications for constrained meshes, Computer Graphics Forum 32 (2pt1) (2013) 11–20. arXiv:https://onlinelibrary.wiley.com/doi/pdf/10.1111/cgf.12021, doi:10.1111/cgf.12021.
URL https://onlinelibrary.wiley.com/doi/abs/10.1111/cgf.12021

[42] C. Tang, X. Sun, A. Gomes, J. Wallner, H. Pottmann, Form-finding with polyhedral meshes made simple, in: ACM SIGGRAPH 2015 Posters, ACM, 2015, p. 5. doi:https://doi.org/10.1145/2601097.2601213.

[43] H. Pottmann, Y. Liu, J. Wallner, A. Bobenko, W. Wang, Geometry of multi-layer freeform structures for architecture, ACM Transactions on Graphics (TOG) 26 (3) (2007) 65. doi:https://doi.org/10.1145/1276377.1276458.

[44] R. Mesnil, C. Douthe, O. Baverel, Non-standard patterns for gridshell structures: Fabrication and structural optimization, Journal of the International Association for Shell and Spatial Structures 58 (4) (2017) 277–286. doi:https://doi.org/10.20898/j.iass.2017.194.893.

[45] J. C. Maxwell, I.—on reciprocal figures, frames, and diagrams of forces, Earth and Environmental Science Transactions of the Royal Society of Edinburgh 26 (1) (1870) 1–40. doi:https://doi.org/10.1080/14786446408643663.

[46] A. McRobie, Maxwell and rankine reciprocal diagrams via minkowski sums for two-dimensional and three-dimensional trusses under load, International Journal of Space Structures 31 (2-4) (2016) 203–216. doi:https://doi.org/10.1177/0266351116660800.

[47] H. Schober, Geometrie-prinzipien für wirtschaftliche und effiziente schalentragwerke (teil 1), Bautechnik 79 (1) (2002) 16–24. doi:https://doi.org/10.1002/bate.200200030.

[48] R. Mesnil, C. Douthe, O. Baverel, B. Léger, J.-F. Caron, Isogonal moulding surfaces: A family of shapes for high node congruence in free-form structures, Automation in Construction 59 (2015) 38 – 47. doi:https://doi.org/10.1016/j.autcon.2015.07.009.
URL http://www.sciencedirect.com/science/article/pii/S0926580515001521

Appendix A. Demonstration of the set of inequations (3)

We prove here Eq. 3 by first proving the direct implication and then its converse.

$\boxed{\Longrightarrow}$ To prove the direct implication, suppose that the block is translationally interlocked. We want to prove inequalities (i), (ii) and (iii) of Eq. 3.

Since the block is translationally interlocked, according to Eq. 1, for all $\vec{u}$, there exists $i \in \{1,2,3,4\}$ such that $\vec{u}.\vec{n}_i < 0$. This inequality being true for all $\vec{u}$, choosing an appropriate vector $\vec{u}$ allows to prove the inequalities (i), (ii) and (iii). Indeed, suppose $\vec{u} = det\,(\vec{n}_1,\vec{n}_2,\vec{n}_3) \cdot (\vec{n}_1 \times \vec{n}_2)$. This vector is one vector of the basis $\mathfrak{B}$ mentioned earlier. The dot product of this vector with the plane normals thus gives:

$$\left\{\begin{array}{lcll} \vec{u}.\vec{n}_1 & = & 0 & \\ \vec{u}.\vec{n}_2 & = & 0 & \\ \vec{u}.\vec{n}_3 & = & (det\,(\vec{n}_1,\vec{n}_2,\vec{n}_3))^2 & \geq 0 \\ \vec{u}.\vec{n}_4 & = & det\,(\vec{n}_1,\vec{n}_2,\vec{n}_3) \cdot det\,(\vec{n}_1,\vec{n}_2,\vec{n}_4) & \end{array}\right.$$

But we know that there exists $i \in \{1,2,3,4\}$ such that $\vec{u}.\vec{n}_i < 0$. Since the first three values are positives or null, we necessarily have $\vec{u}.\vec{n}_4 < 0$. This means, the inequality (i) of Eq.3 is verified:

$$det\,(\vec{n}_1,\vec{n}_2,\vec{n}_3) \cdot det\,(\vec{n}_1,\vec{n}_2,\vec{n}_4) < 0$$

Similarly, with $\vec{v} = det\,(\vec{n}_2,\vec{n}_3,\vec{n}_1) \cdot (\vec{n}_2 \times \vec{n}_3)$, we have:

$$\left\{\begin{array}{lcll} \vec{v}.\vec{n}_1 & = & (det\,(\vec{n}_2,\vec{n}_3,\vec{n}_1))^2 & \geq 0 \\ \vec{v}.\vec{n}_2 & = & 0 & \\ \vec{v}.\vec{n}_3 & = & 0 & \\ \vec{v}.\vec{n}_4 & = & det\,(\vec{n}_2,\vec{n}_3,\vec{n}_1) \cdot det\,(\vec{n}_2,\vec{n}_3,\vec{n}_4) & \end{array}\right.$$

We necessarily have $\vec{v}.\vec{n}_4 < 0$, which is the inequality (ii) of Eq. 3. Finally, we prove the inequality (iii) of Eq. 3 with $\vec{w} = det\,(\vec{n}_3,\vec{n}_1,\vec{n}_2) \cdot (\vec{n}_3 \times \vec{n}_1)$.

$\boxed{\Longleftarrow}$ To prove the converse, suppose that inequalities (i), (ii) and (iii) of Eq. 3 are true and let us prove that the block is thus necessarily translationally interlocked. For this, let us proceed with a proof by contradiction.

Suppose the block is not translationally interlocked.

Let $\epsilon = det\,(\vec{n}_1,\vec{n}_2,\vec{n}_3)$ and let us express the determinant $det\,(\epsilon \cdot \vec{n}_1 \times \vec{n}_2, \epsilon \cdot \vec{n}_2 \times \vec{n}_3, \epsilon \cdot \vec{n}_3 \times \vec{n}_1)$ as a scalar triple product. A basic derivation shows that

$$det\,(\epsilon \cdot \vec{n}_1 \times \vec{n}_2, \epsilon \cdot \vec{n}_2 \times \vec{n}_3, \epsilon \cdot \vec{n}_3 \times \vec{n}_1) = \epsilon^5$$

Since (i) is true, $\epsilon \neq 0$. Hence,

$$det\,(\epsilon \cdot \vec{n}_1 \times \vec{n}_2, \epsilon \cdot \vec{n}_2 \times \vec{n}_3, \epsilon \cdot \vec{n}_3 \times \vec{n}_1) \neq 0$$

The set $\mathfrak{B} = (\epsilon \cdot \vec{n}_1 \times \vec{n}_2, \epsilon \cdot \vec{n}_2 \times \vec{n}_3, \epsilon \cdot \vec{n}_3 \times \vec{n}_1)$ is therefore linearly independent. Since its length is 3, $\mathfrak{B}$ is a basis of E.

Since the block is not translationally interlocked, according to Eq. 2, there exists $\vec{u}_0$ such that $\vec{u}_0 \cdot \vec{n}_i \geq 0$ for all $i \in \{1,2,3,4\}$. Let us decompose $\vec{u}_0$ over the basis $\mathfrak{B}$.

Let $A, B, C \in \mathbb{R}$, not simultaneously zero, such that

$$\vec{u}_0 = A\,\epsilon\,\vec{n}_1 \times \vec{n}_2 + B\,\epsilon\,\vec{n}_2 \times \vec{n}_3 + C\,\epsilon\,\vec{n}_3 \times \vec{n}_1$$

Hence,

$$\left\{\begin{array}{lcl} \vec{u}_0 \cdot \vec{n}_1 & = & B\,\epsilon\,(\vec{n}_2 \times \vec{n}_3) \cdot \vec{n}_1 = B\,\epsilon\,det\,(\vec{n}_1,\vec{n}_2,\vec{n}_3) = B \cdot \epsilon^2 \\ \vec{u}_0 \cdot \vec{n}_2 & = & C\,\epsilon\,(\vec{n}_3 \times \vec{n}_1) \cdot \vec{n}_2 = C\,\epsilon\,det\,(\vec{n}_1,\vec{n}_2,\vec{n}_3) = C \cdot \epsilon^2 \\ \vec{u}_0 \cdot \vec{n}_3 & = & A\,\epsilon\,(\vec{n}_1 \times \vec{n}_2) \cdot \vec{n}_3 = A\,\epsilon\,det\,(\vec{n}_1,\vec{n}_2,\vec{n}_3) = A \cdot \epsilon^2 \\ \vec{u}_0 \cdot \vec{n}_4 & = & A\,\epsilon\,(\vec{n}_1 \times \vec{n}_2) \cdot \vec{n}_4 + B\,\epsilon\,(\vec{n}_2 \times \vec{n}_3) \cdot \vec{n}_4 + C\,\epsilon\,(\vec{n}_3 \times \vec{n}_1) \cdot \vec{n}_4 \end{array}\right.$$

But, for all $i \in \{1,2,3,4\}$, $\vec{u}_0 \cdot \vec{n}_i \geq 0$. Hence, $A \geq 0$, $B \geq 0$ et $C \geq 0$. Rewriting the fourth inequality ($\vec{u}_0 \cdot \vec{n}_4 \geq 0$):

$$\begin{array}{rcl} \vec{u}_0 \cdot \vec{n}_4 & = & A\,\epsilon\,(\vec{n}_1 \times \vec{n}_2) \cdot \vec{n}_4 + B\,\epsilon\,(\vec{n}_2 \times \vec{n}_3) \cdot \vec{n}_4 + C\,\epsilon\,(\vec{n}_3 \times \vec{n}_1) \cdot \vec{n}_4 \\ & = & A\,det\,(\vec{n}_1,\vec{n}_2,\vec{n}_3)\;det\,(\vec{n}_1,\vec{n}_2,\vec{n}_4) \\ & & \quad +B\,det\,(\vec{n}_1,\vec{n}_2,\vec{n}_3)\;det\,(\vec{n}_2,\vec{n}_3,\vec{n}_4) \\ & & \quad\quad +C\,det\,(\vec{n}_1,\vec{n}_2,\vec{n}_3)\;det\,(\vec{n}_3,\vec{n}_1,\vec{n}_4) \\ & = & T_1 + T_2 + T_3 \end{array}$$

with

$$\begin{array}{rcl} T_1 & = & A\,det\,(\vec{n}_1,\vec{n}_2,\vec{n}_3)\;det\,(\vec{n}_1,\vec{n}_2,\vec{n}_4) \\ T_2 & = & B\,det\,(\vec{n}_1,\vec{n}_2,\vec{n}_3)\;det\,(\vec{n}_2,\vec{n}_3,\vec{n}_4) \\ T_3 & = & C\,det\,(\vec{n}_1,\vec{n}_2,\vec{n}_3)\;det\,(\vec{n}_3,\vec{n}_1,\vec{n}_4) \end{array}$$

Thus

$$\vec{u}_0 \cdot \vec{n}_4 \geq 0 \quad \Leftrightarrow \quad T_1 + T_2 + T_3 \geq 0 \qquad \text{(A.1)}$$

Since $A \geq 0$, $B \geq 0$ and $C \geq 0$, inequalities (i), (ii) and (iii) from Eq. 3 result therefore in $T_1 \leq 0$, $T_2 \leq 0$ and $T_3 \leq 0$. Hence, $T_1 + T_2 + T_3 \leq 0$. Hence, since Eq. A.1:

$$T_1 + T_2 + T_3 = 0$$

T_1, T_2 and T_3 have the same sign, therefore:

$$T_1 = T_2 = T_3 = 0$$

T_1 is the product of $A \geq 0$ and a quantity strictly negative (from inequality (i) of Eq. 3). Thus $A = 0$. Similarly, with T_2 and T_3 we get $B = 0$ and $C = 0$.

But

$$\vec{u}_0 = A\,\epsilon\,\vec{n}_1 \times \vec{n}_2 + B\,\epsilon\,\vec{n}_2 \times \vec{n}_3 + C\,\epsilon\,\vec{n}_3 \times \vec{n}_1$$

Hence $\vec{u}_0 = 0$, what is impossible because $\vec{u}_0$ could not be the zero vector. We have been supposing that the block is translationally interlocked and get a contradiction. Therefore, the block is necessarily translationally interlocked.